



HAL
open science

The Blasius equation

Augustin Fruchard, Bernard Brighi, Tewfik Sari

► **To cite this version:**

| Augustin Fruchard, Bernard Brighi, Tewfik Sari. The Blasius equation. 2010. hal-00493860

HAL Id: hal-00493860

<https://hal.science/hal-00493860v1>

Submitted on 8 Nov 2010

HAL is a multi-disciplinary open access archive for the deposit and dissemination of scientific research documents, whether they are published or not. The documents may come from teaching and research institutions in France or abroad, or from public or private research centers.

L'archive ouverte pluridisciplinaire **HAL**, est destinée au dépôt et à la diffusion de documents scientifiques de niveau recherche, publiés ou non, émanant des établissements d'enseignement et de recherche français ou étrangers, des laboratoires publics ou privés.

The Blasius equation

Bernard BRIGHI, Augustin FRUCHARD and Tewfik SARI

June 14, 2010

Abstract. The Blasius problem $f''' + ff'' = 0$, $f(0) = -a$, $f'(0) = b$, $f'(+\infty) = \lambda$ is investigated, in particular in the difficult and scarcely studied case $b < 0 \leq \lambda$. The shape and the number of solutions are determined. The method is first to reduce to the Crocco equation $uu'' + s = 0$ and then to use an associated autonomous planar vector field. The most useful properties of Crocco solutions appear to be related to canard solutions of a slow fast vector field.

KEYWORDS : Blasius equation, Crocco equation, boundary value problem on infinite interval, canard solution.

1 Introduction

This is the report of a talk given in *Rencontre du réseau Georges Reeb à la mémoire d'Emmanuel Isambert*, Paris, December 21 - 22, 2007.

We present in this article a selection of results of [6]. The reader is referred to [6] for complete proofs, additional and intermediate results. We take the occasion to completely change the order of presentation: in [6] we first give the results on the Blasius equation with a sketch of proof, then we introduce the Crocco equation and the vector field, we establish results and proofs on these intermediate equations and then we return to the proof of the initial result. Here we choose a different order and we postpone the main result at the end of the article. We hope that this article may be a first approach before a thorough study of [6].

The paper is organized as follows. In Section 2, we state the main problem of the paper which is the investigation of the following *Blasius Boundary Value Problem* (BBVP for short)

$$f''' + ff'' = 0 \quad \text{on } [0, +\infty[, \quad (1)$$

$$f(0) = -a, \quad f'(0) = b, \quad \lim_{t \rightarrow +\infty} f'(t) = \lambda. \quad (2)$$

We list some former results, according to the relative values of b and λ , and we focus our attention on the case $b < 0 \leq \lambda$, which is our case of interest. In Section 3, we show that, in the latter case, this boundary value problem is equivalent to the *Crocco Boundary Value Problem* (CBVP)

$$\begin{cases} uu'' + s = 0 & \text{on } [b, \lambda[, \\ u'(b) = a, \quad \lim_{s \rightarrow \lambda} u(s) = 0. \end{cases} \quad (3)$$

where $[b, \lambda[$ appears as the maximal right-interval of definition of the solution. In Section 4, we show that the similarity properties of the Blasius or

the Crocco solutions permit to reduce the non autonomous second order differential equation of Crocco to an autonomous planar vector and we notice that the maximal right-interval of definition of the solutions of the Crocco equation presents a discontinuity with respect to the initial condition. It is well known that the maximal right-interval of definition of the solution of a differential equation is not continuous in general with respect to the initial conditions. It is simply lower semicontinuous. Actually, in Section 6, we see that the solutions of the Crocco differential equation which are close to 0 for s close to 0 are *canard* solutions of a slow-fast vector field. These solutions play an important role in the description of the discontinuity of the maximal right-interval of definition of the solution of the Crocco equation. In Section 7, we analyze this discontinuity which occurs along a particular orbit of the planar vector field considered in Section 4. In Section 8, we give a lower bound of the number of solutions of the boundary value problem associated to the Blasius equation, in the case $b < 0 \leq \lambda$. In Section 9, we describe a difficulty encountered in numerical simulations. Indeed, due to the canard solutions phenomenon, some solutions of the Crocco equation become exponentially small for $s < 0$ and the numerical scheme cannot give the right solution. We show how to use the theoretical study in Section 5 to overcome this difficulty.

2 The Blasius Boundary Value Problem

The Blasius Boundary Value Problem (1-2) arises for the first time, with $a = b = 0$ and $\lambda = 2$, in 1907 in the thesis of Blasius [3, 4]. In the case $a = b = 0$, Hermann Weyl [16] proves that the BBVP has one and only one solution. The proof is very elementary but strongly uses the fact that $a = b = 0$, see also [5, 8]. The BBVP plays a central role in fluid mechanics [12]: The Blasius equation (1) was obtained using a similarity transform and enabled successful treatment of the laminar boundary layer on a flat plate. Since equation (1) can be seen as a first order linear differential equation for f'' , we have

$$f''(t) = f''(0) \exp \left\{ - \int_0^t f(\tau) d\tau \right\}.$$

Hence, the BBVP splits into three cases, called respectively linear, concave and convex:

- If $\lambda = b$, then the BBVP has a unique solution, given by $f(t) = bt - a$.
- If $\lambda > b$, then any possible solution must satisfy $f''(t) > 0$ for all $t \geq 0$, i.e. has to be convexe.
- If $\lambda < b$, then possible solutions are concave.

The concave case is completely solved and well-known [1].

Proposition 1 — In the case $\lambda < b$, the BBVP (1-2) has exactly one solution if $0 \leq \lambda < b$, and no solution if $\lambda < 0$.

When $b \geq 0$, the convex case $\lambda > b$ is also well-known, see [8].

Proposition 2 ([6] Corollary 3.6) — The BBVP (1-2), where $b \geq 0$ and $\lambda > b$, has exactly one solution when $a \leq 0$ or $b > 0$. When $a > 0$ and $b = 0$, the BBVP has exactly one solution for all $\lambda > a^2\lambda_+$ and no solution if $0 < \lambda \leq a^2\lambda_+$, where $\lambda_+ \simeq 1.304$ is defined in Proposition 5.

We know that every solution of the Blasius equation (1) such that $f''(0) > 0$ is defined for all t and its derivative has a finite and non-negative limit as $t \rightarrow +\infty$ ([6] Proposition 3.1). Thus

Proposition 3 — The BBVP (1-2) has no solution if $b < \lambda < 0$.

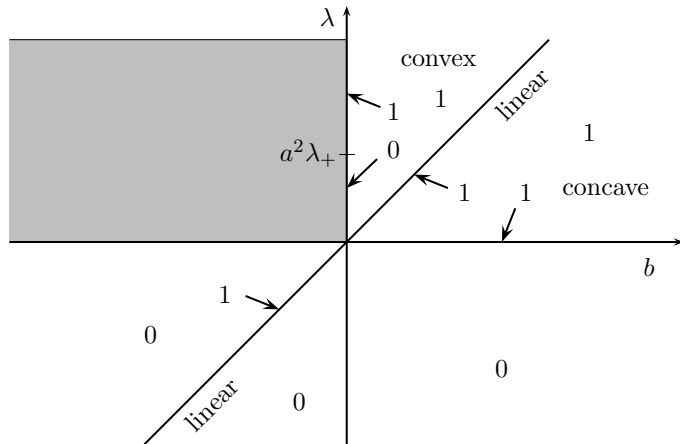


Figure 1: In the plane (b, λ) , the number of solutions of the BBVP (5) in each region and on their border. In gray, the remaining region to investigate, purpose of this article.

In this article, we focus on the remaining case $b < 0 \leq \lambda$, which is much richer and trickier. Non uniqueness for the BBVP is mentioned in the literature, but either only supported by numerical investigations [9], or with incomplete proofs [10, 13].

The Blasius equation (1) has the following similarity property:

$$\text{If } t \mapsto f(t) \text{ is a solution of (1), so is } t \mapsto \sigma f(\sigma t), \text{ for all } \sigma \in \mathbb{R}. \quad (4)$$

This allows us to restrict our attention without loss of generality to the case $b = -1$, i.e. to the BBVP

$$\begin{cases} f''' + f f'' = 0 & \text{on } [0, +\infty[, \\ f(0) = -a, \quad f'(0) = -1, \quad \lim_{t \rightarrow +\infty} f'(t) = \lambda \geq 0. \end{cases} \quad (5)$$

The purpose of this article is to count the number of solutions of (5). The main result, at the end of Section 8, gives a minimum number of solutions of (5) depending on the values of a and λ . We conjecture that this minimum number is the exact number of solutions.

3 The Crocco Boundary Value Problem

Since $f'' > 0$ it follows that $t \mapsto f'(t)$ is a diffeomorphism. Hence we can use f' as an independent variable and express f'' as a function of f' . This is the so-called *Crocco transformation* [7]

$$s = f', \quad f'' = u(s)$$

Differentiating $f'' = u(f')$ we obtain $u'(s) = -f$. Differentiating once again we obtain $u''(s)u(s) = -s$. Thus the Blasius equation (1) is equivalent to the Crocco differential equation

$$u''u + s = 0 \quad (6)$$

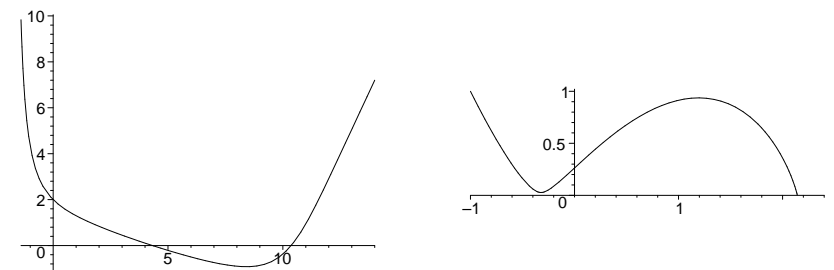


Figure 2: On the left, the Blasius solution $t \mapsto f(t; -2, 1)$; on the right, the corresponding Crocco solution $s \mapsto u(s; -2, 1)$.

As we will see, the BBVP (5) is equivalent to the Crocco Boundary Value Problem (3) for $b = -1$, rewritten below for convenience

$$\begin{cases} u u'' + s = 0 & \text{on } [-1, \lambda[, \\ u'(-1) = a, \quad \lim_{s \rightarrow \lambda} u(s) = 0. \end{cases} \quad (7)$$

The equivalence between (5) and (7) will become clear after the following remarks. In order to solve (5) we use the *shooting method*. Let $f(\cdot; a, c)$ denote the solution of the Blasius Initial Value Problem (BIVP)

$$f''' + ff'' = 0, \quad f(0) = -a, \quad f'(0) = -1, \quad f''(0) = c > 0. \quad (8)$$

The solution $f(\cdot; a, c)$ is defined for all $t \geq 0$ and its derivative has a finite and non-negative limit as $t \rightarrow +\infty$ ([6] Proposition 3.1). Let $\mathcal{L}(a, c)$ denote the limit¹

$$\mathcal{L}(a, c) := \lim_{t \rightarrow +\infty} f'(t; a, c) \geq 0. \quad (9)$$

Then ([6] Proposition 2.1), $[-1, \mathcal{L}(a, c)[$ is the maximal right interval of existence of the solution $u(\cdot; a, c)$ of the Crocco Initial Value Problem (CIVP)

$$uu'' + s = 0, \quad u(-1) = c > 0, \quad u'(-1) = a. \quad (10)$$

See Figure 2 for a comparison between a Blasius solution and the corresponding Crocco solution.

Moreover, we have

$$\lim_{s \rightarrow \mathcal{L}(a, c)} u(s) = 0 \quad \text{and} \quad (\mathcal{L}(a, c) > 0 \Rightarrow \lim_{s \rightarrow \mathcal{L}(a, c)} u'(s) = -\infty)$$

This shows that (5) is equivalent to (7).

4 Use of symmetries to reduce the order

The similarity property (4) is rewritten as follows for the Crocco equation (6)

$$\text{If } \sigma > 0 \text{ and } s \mapsto u(s) \text{ is a solution of (6), so is } u^\sigma : s \mapsto \sigma^3 u(\sigma^{-2}s). \quad (11)$$

This similarity property reduces the Crocco equation (6) to a system of autonomous differential equations. Actually, the change of variables

$$x(s) = (-s)^{-1/2} u'(s), \quad y(s) = (-s)^{-3/2} u(s)$$

leads to the system

$$x' = \frac{1}{2} \frac{x + \frac{1}{y}}{-s}, \quad y' = \frac{x + \frac{3}{2} y}{-s}.$$

Thus, using the change of independent variable $s = -e^{-\tau}$, we obtain the planar vector field

$$\dot{x} = \frac{1}{2} x + \frac{1}{y}, \quad \dot{y} = x + \frac{3}{2} y, \quad (12)$$

¹This function \mathcal{L} is denoted by $\tilde{\Lambda}$ in [6].

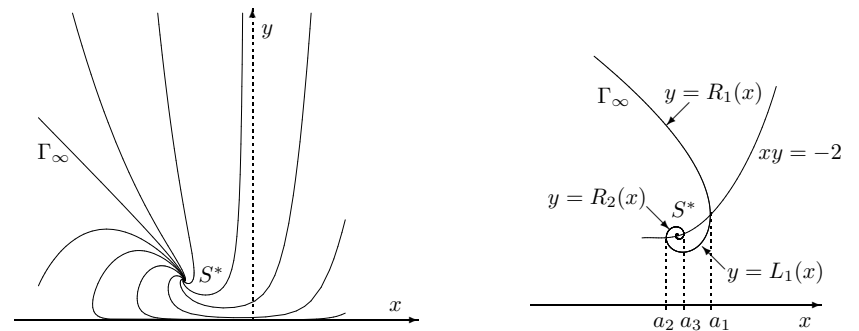


Figure 3: On the left: the phase portrait of (12). On the right: sketch of enlargement of Γ_∞ near S^* . The functions L_n and R_n are defined in Section 7.

where the dot is for differentiating with respect to the new independent variable τ . The initial conditions $u(-1) = c$, $u'(-1) = a$ in the CIVP (10) correspond to

$$x(0) = a, \quad y(0) = c.$$

Notice that this vector field describes the Crocco equation (6) only for $s < 0$, since τ tends to $+\infty$ as s tends to 0.

Because the transformation $u \mapsto u^\sigma$ given by (11) corresponds to the shift $\tau \mapsto \tau + 2 \ln \sigma$, to each orbit $\{(x(\tau), y(\tau)); \tau \in \mathbb{R}\}$ of a solution of (12) corresponds a whole family $(u^\sigma)_{\sigma > 0}$ of solutions of (6) connected by the similarity (11). In particular, the unique stationary point $S^* = (-\sqrt{3}, \frac{2}{\sqrt{3}})$ of (12) corresponds to the unique self-similar positive solution u_* of (6), *i.e.* satisfying $u_*(s) = \sigma^3 u_*(\sigma^{-2}s)$ for $s < 0 < \sigma$, namely

$$u_*(s) = \frac{2}{\sqrt{3}} (-s)^{3/2}. \quad (13)$$

A study of this vector field, detailed in [6], shows the following.

- All solutions of (12) are defined on \mathbb{R} and tend to S^* as $\tau \rightarrow -\infty$.
- There is one and only one orbit, denoted by Γ_∞ , such that any solution (x, y) parametrizing Γ_∞ satisfies that $\frac{x(\tau)}{y(\tau)}$ tends to -1 as $\tau \rightarrow +\infty$, see Figure 3.
- For all solutions $(x(\tau), y(\tau))$ except those on $\Gamma_\infty \cup \{S^*\}$, the quotient $\frac{x(\tau)}{y(\tau)}$ tends to 0 as $\tau \rightarrow +\infty$.
- ([6] Theorem 2.4) For all solutions $(x(\tau), y(\tau))$ except those on $\Gamma_\infty \cup \{S^*\}$, $\frac{x(\tau)^3}{y(\tau)}$ has a limit $k \in \mathbb{R}$ as $\tau \rightarrow +\infty$. The number k parametrizes

the orbit of (12) denoted by Γ_k . In terms of positive Crocco solutions, we have the following properties:

1. if $(a, c) \in \Gamma_\infty$ then $\lim_{s \rightarrow 0^-} u(s; a, c) = 0$ and $\lim_{s \rightarrow 0^-} u'(s; a, c) < 0$,
2. if $(a, c) = S^*$ then $\lim_{s \rightarrow 0^-} u(s; a, c) = 0$ and $\lim_{s \rightarrow 0^-} u'(s; a, c) = 0$,
3. Otherwise $(a, c) \in \Gamma_k$ for some $k \in \mathbb{R}$. In that case, $u(0; a, c) > 0$ and $u'(0; a, c)$ is of the same sign as k .

Let (a, c) be an initial condition which is close to Γ_∞ . If (a, c) lies on

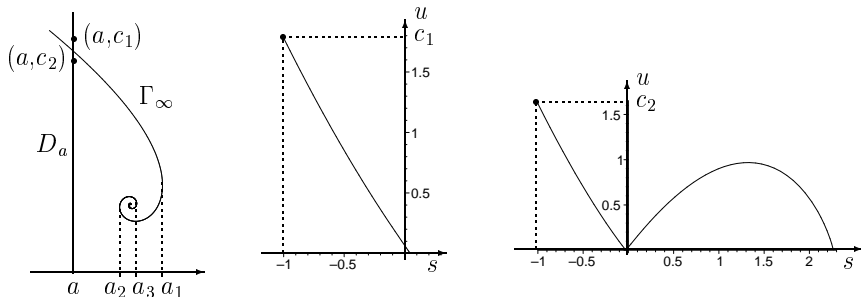


Figure 4: A sketch of the spiral Γ_∞ and two numerical Crocco solutions with initial conditions $u_1(-1) = c_1 = 1.78$, $u_1'(-1) = a = -2$ and $u_2(-1) = c_2 = 1.62$, $u_2'(-1) = a = -2$, where (a, c_1) and (a, c_2) are on the convex and on the concave sides of Γ_∞ respectively.

the convex side of Γ_∞ , then $u(0; a, c)$ is close to 0 and $u'(0; a, c) < 0$. Since $u(s; a, c)$ becomes concave for $s > 0$, it follows that $\mathcal{L}(a, c)$ is close to 0. If (a, c) lies on the concave side of Γ_∞ , then $u(0; a, c)$ is small and $u'(0; a, c) > 0$. Thus $\mathcal{L}(a, c)$ is not close to 0, see Figure 4. This shows that the function $\mathcal{L}(a, c)$ is discontinuous on Γ_∞ . The precise description of this discontinuity needs the knowledge of the behavior of the solutions $u(s)$ of the Crocco equation (6) for which $u(0)$ is close to 0. This behavior is described in the following section.

5 Crocco solutions near $u = 0$...

The following result describes Crocco solutions close to 0 and with positive slope for $s = 0$: they take an exponentially small value at some small negative abscissa of s and then go far from the s axis.

Proposition 4 — Fix $\alpha > 0$ and let $0 < \varepsilon \rightarrow 0$. Let $u = u(s, \varepsilon)$ denote the solution of (6) such that $u(0, \varepsilon) = \varepsilon$ and $u'(0, \varepsilon) = \alpha$. Then $u(s, \varepsilon)$ reaches

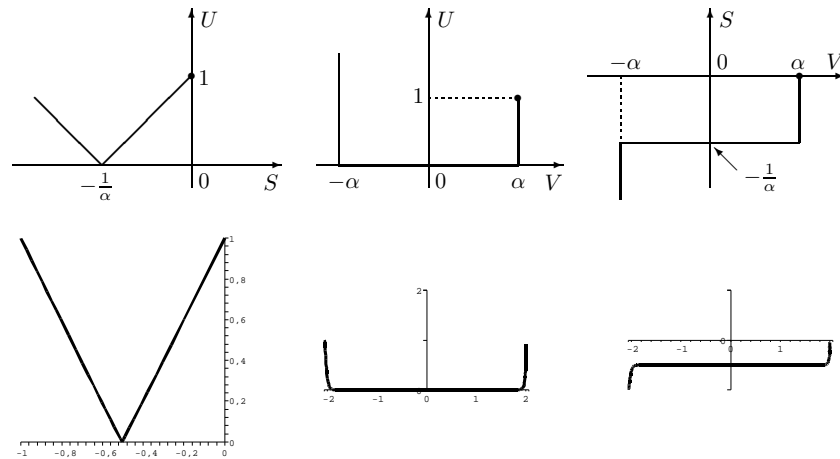


Figure 5: Above: schematic graphs of the solution of (14) in the limit $\varepsilon \rightarrow 0$, respectively in the variables S, U , the variables U, V and S, V . Below: the numerical solution corresponding to $\varepsilon = 0.1$ and $\alpha = 2$.

its minimum at some abscissa $s = \kappa(\varepsilon) < 0$ satisfying $\kappa(\varepsilon) = -\frac{\varepsilon}{\alpha}(1 + o(1))$ and

$$u(\kappa(\varepsilon), \varepsilon) = \exp\left(-\frac{\alpha^3}{2\varepsilon}(1 + o(1))\right) \quad \text{as } \varepsilon \rightarrow 0.$$

Moreover, for all $B < 0$ fixed, we have $u(\varepsilon s, \varepsilon) = \varepsilon(|\alpha s + 1| + o(1))$ as $\varepsilon \rightarrow 0$, uniformly for $s \in [B, 0]$.

Proof. The reference [6] contains two proofs: one in Section 5 and an alternative one in Section 6. We give here an overview of the second one. The solution $u(s, \varepsilon)$ is defined for all $s \leq 0$ and is positive. The function $U(S, \varepsilon)$, defined by

$$U(S, \varepsilon) = \frac{1}{\varepsilon} u(\varepsilon S, \varepsilon),$$

is the solution of the initial value problem

$$U \frac{d^2 U}{dS^2} + \varepsilon S = 0, \quad U(0) = 1, \quad \frac{dU}{dS}(0) = \alpha. \quad (14)$$

Except near the axis $U = 0$, and for bounded values of S , U'' is close to 0, *i.e.* the solutions are almost affine. Precisely, one has for all fixed $S_0 \in]-\frac{1}{\alpha}, 0]$

$$U(S, \varepsilon) = \alpha S + 1 + o(1) \quad \text{as } \varepsilon \rightarrow 0, \quad \text{uniformly for } S \in [S_0, 0] \quad (15)$$

What is less obvious is that this approximation is still valid up to $-\frac{1}{\alpha}$ and that, for any fixed $B \leq -\frac{1}{\alpha}$, the solution satisfies the approximation

$U(S, \varepsilon) = -\alpha S - 1 + o(1)$ uniformly for $B \leq S \leq -\frac{1}{\alpha}$. In other words, after its passage near the axis, the solution $U(S, \varepsilon)$ behaves like a light ray reflecting on a mirror, see Figure 5. To see this, we use the new variable $W = \varepsilon \ln U$ and we choose $V = \frac{dU}{dS}$ as an independent variable; we obtain

$$\frac{dS}{dV} = -\frac{e^{W/\varepsilon}}{\varepsilon S}, \quad \frac{dW}{dV} = -\frac{V}{S}. \quad (16)$$

In a interval where $W < 0$ and $S < 0$, we have $\lim_{\varepsilon \rightarrow 0} \frac{e^{W/\varepsilon}}{\varepsilon S} = 0$. Thus (16) is a regular perturbation of

$$\frac{dS}{dV} = 0, \quad \frac{dW}{dV} = -\frac{V}{S}.$$

Since S is close to $-\frac{1}{\alpha}$ when U is close to 0, we deduce that

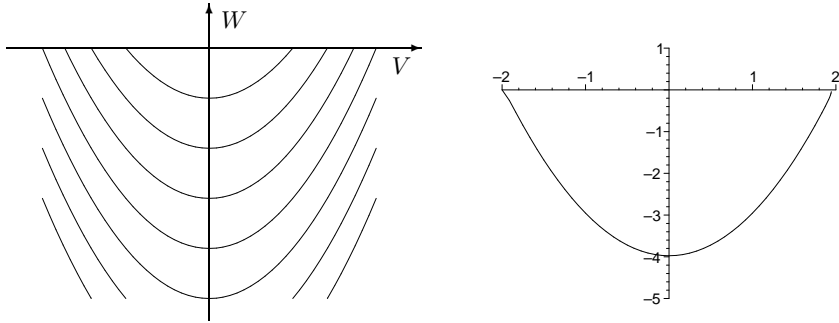


Figure 6: On the left, a scheme of the vector field in the variables V, W . On the right, the numerical solution corresponding to $\varepsilon = 0.1$ and $\alpha = -2$.

$$S(V, \varepsilon) = -\frac{1}{\alpha} + o(1), \quad W(V, \varepsilon) = \frac{\alpha V^2}{2} + W_0 + o(1) \quad \text{as } \varepsilon \rightarrow 0, \quad (17)$$

uniformly for $V \in [-V_0, V_0]$, where $W_0 < 0$ and $V_0 < \sqrt{-2W_0/\alpha}$, see Figure 6, left. With the condition $W(\alpha, \varepsilon) = o(1)$, we obtain $W_0 = -\frac{\alpha^3}{2} + o(1)$. Thus we have

$$S(V, \varepsilon) = -\frac{1}{\alpha} + o(1), \quad W(V, \varepsilon) = \alpha \frac{V^2 - \alpha^2}{2} + o(1) \quad \text{as } \varepsilon \rightarrow 0,$$

uniformly for $V \in [-A_0, A_0]$, where A_0 can be chosen as close to α as we want. Hence we have

$$U(V, \varepsilon) = o(1) \quad \text{uniformly for } V \in [-A_0, A_0]. \quad (18)$$

The minimum of $U(S, \varepsilon)$ is reached for $S = K(\varepsilon)$ which corresponds to $V = 0$. Hence

$$K(\varepsilon) = -\frac{1}{\alpha} + o(1), \quad U(K(\varepsilon), \varepsilon) = \exp\left(\frac{W(0, \varepsilon)}{\varepsilon}\right) = \exp\left(-\frac{\alpha^3 + o(1)}{2\varepsilon}\right).$$

Thus $\kappa(\varepsilon) = \varepsilon K(\varepsilon) = \varepsilon\left(-\frac{1}{\alpha} + o(1)\right)$ and, using $\varepsilon = \exp\frac{\varepsilon \ln \varepsilon}{\varepsilon} = \exp\frac{o(1)}{\varepsilon}$, we have

$$u(\kappa(\varepsilon), \varepsilon) = \varepsilon U(K(\varepsilon), \varepsilon) = \varepsilon \exp\left(-\frac{\alpha^3 + o(1)}{2\varepsilon}\right) = \exp\left(-\frac{\alpha^3 + o(1)}{2\varepsilon}\right).$$

Using again the differential equation in (14), we have $V(S, \varepsilon) = -\alpha + o(1)$ uniformly for $S \in [B, S_1]$, where $B < S_1$ and S_1 is as close to $-\frac{1}{\alpha}$ as we want. Thus

$$U(S, \varepsilon) = -\alpha \left(S + \frac{1}{\alpha}\right) + o(1), \quad \text{uniformly for } S \in [S_2, S_1]. \quad (19)$$

Using (15) and (19), together with (18) we conclude that

$$U(S, \varepsilon) = |\alpha S + 1| + o(1) \quad \text{uniformly for } S \in [S_2, 0].$$

Hence $u(\varepsilon S, \varepsilon) = \varepsilon(|\alpha S + 1| + o(1))$ uniformly for $S \in [B, 0]$, as $\varepsilon \rightarrow 0$. \square

6 ... are canard solutions!

The solution $U(V, \varepsilon)$ considered in the proof of Proposition 4 is a canard solution. Indeed, $(S(V, \varepsilon), U(V, \varepsilon))$ is a solution of the slow fast system

$$\varepsilon \frac{dS}{dV} = -\frac{U}{S}, \quad \varepsilon \frac{dU}{dV} = -\frac{VU}{S}. \quad (20)$$

whose slow manifold $U = 0$ is attractive when $V < 0$ and repulsive when $V > 0$. Notice that

$$S(V) = \text{constant} < 0, \quad U(V) = 0, \quad (21)$$

are canard solutions of (20) since they are on the attractive part of the slow manifold when $V < 0$ and on its repulsive part when $V > 0$. These solutions do not correspond to actual solutions of the differential equation in (14) since the latter are for $U \neq 0$.

Considered as a system in \mathbb{R}^3 , (20) is a slow-fast system with two fast variables S and U and one slow variable V . However, it is possible to rewrite it as a system with two slow variables and only one fast. Actually $T = VS - U$ is a slow variable. With this variable, (20) becomes

$$\varepsilon \frac{dS}{dV} = \frac{T - VS}{S}, \quad \frac{dT}{dV} = S. \quad (22)$$

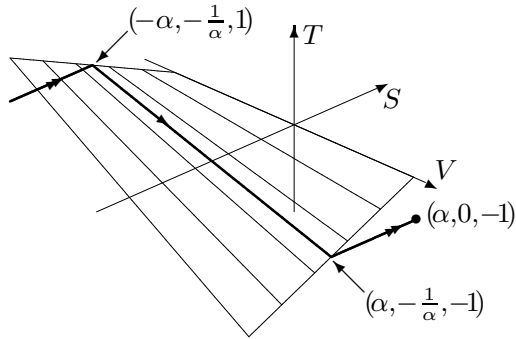


Figure 7: *The canard of (22).*

This is a singularly perturbed system whose slow manifold is the surface $T = VS$. This slow manifold is attractive for $V < 0$ and repulsive for $V > 0$. The Tikhonov theorem (see [14, 11] and [15] Section 39) describes the behavior of the solution $(S(V, \varepsilon), T(V, \varepsilon))$ of (22) when $V > 0$. There is a fast transition (see Figure 7) taking the trajectory $(V, S(V, \varepsilon), T(V, \varepsilon))$, from its initial point $(\alpha, 0, -1)$, to a $o(1)$ neighborhood of the point $(\alpha, -\frac{1}{\alpha}, -1)$ of the slow manifold, preceded by a slow transition near a solution $(-\frac{1}{\alpha}, -\frac{V}{\alpha})$ of the reduced problem

$$S = \frac{T}{V}, \quad \frac{dT}{dV} = S.$$

More precisely, for any A_0 and A_1 , such that $0 < A_1 < A_0 < \alpha$, we have

$$S(V, \varepsilon) = -\frac{1}{\alpha} + o(1) \quad \text{uniformly for } V \in [A_1, A_0], \quad (23)$$

$$T(V, \varepsilon) = -\frac{V}{\alpha} + o(1) \quad \text{uniformly for } V \in [A_1, \alpha].$$

Notice that A_0 (resp. A_1) is fixed but may be chosen as close to α (resp. 0), as we want. The approximation for S does not hold near $V = \alpha$ since there is a boundary layer (fast transition) from $S = 0$ at $V = \alpha$ to $S = -\frac{1}{\alpha}$ for V close to α . We deduce that

$$U(V, \varepsilon) = VS(V, \varepsilon) - T(V, \varepsilon) = o(1), \quad \text{uniformly for } V \in [A_1, \alpha]. \quad (24)$$

A priori, Tikhonov theorem does not apply for $V \leq 0$, because for $V = 0$ the slow manifold becomes repulsive, but we will see that (24) still holds for negative values of V . This is the so-called bifurcation delay [2]. The slow manifold is foliated by the explicit solutions $S(V) = S_0 = \text{constant}$, $T(V) = VS_0$, corresponding to the solutions (21). These solutions are canard solutions since they follow the attractive part and then the repulsive part of the slow manifold, see Figure 7. Knowing the “exit” value $V = \alpha$ of the

solution $T(V, \varepsilon)$ in a small neighborhood of the slow manifold, we want to compute now the “entry” value for which the solution was far from the slow manifold. Since $U = VS - T > 0$, we use the change of variable $W = \varepsilon \ln U$ which proves that the “entry” of the solution in the neighborhood of the slow manifold holds asymptotically for $V = -\alpha$, as shown in the proof of Proposition 4. For details and complements see [6] Section 6.

7 The discontinuity of the function \mathcal{L}

Two particular solutions of the Crocco equation (6) play an important role in our study.

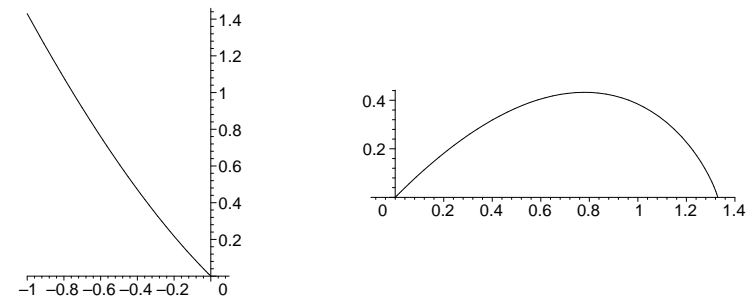


Figure 8: *The graphs of u_- on the left and of u_+ on the right.*

Proposition 5 ([6] Theorem 2.2) — *The Crocco equation (6) has two solutions, denoted by u_- and u_+ such that u_- is the unique solution of (6) satisfying*

$$\lim_{s \rightarrow 0^-} u_-(s) = 0, \quad \lim_{s \rightarrow 0^-} u'_-(s) = -1$$

and u_+ is the unique solution of (6) satisfying

$$\lim_{s \rightarrow 0^+} u_+(s) = 0, \quad \lim_{s \rightarrow 0^+} u'_+(s) = 1.$$

The solution u_- is defined on $] -\infty, 0[$ and the solution u_+ is defined on $] 0, \lambda_+[$ for some $\lambda_+ > 0$.

Numerical computations give $\lambda_+ \approx 1.303918$. See Figure 8 for the graphs of u_- and u_+ .

The orbit Γ_∞ on which \mathcal{L} is discontinuous (See Figure 4 for an illustration of this discontinuity) is given by

$$\Gamma_\infty = \left\{ m(s) = \left((-s)^{-1/2} u'_-(s), (-s)^{-3/2} u_-(s) \right) ; s < 0 \right\}.$$

A consequence of Proposition 4 is the following; see [6] Section 5.2 for the proofs.

Proposition 6 — For every sequence $((\alpha_n, \gamma_n))_{n \in \mathbb{N}}$ which tends to $m(-1)$, the sequence $(u'(0; \alpha_n, \gamma_n))_{n \in \mathbb{N}}$ is bounded and has at most two cluster points: 1 and -1 . Precisely, if (α_n, γ_n) tends to $m(-1)$ on the convex side then $u'(0; \alpha_n, \gamma_n)$ tends to -1 , and if (α_n, γ_n) tends to $m(-1)$ on the concave side then $u'(0; \alpha_n, \gamma_n)$ tends to 1.

Remark — This statement seems to contradict the well-known property of continuity with respect to initial conditions: if (a_1, c_1) and (a_2, c_2) are two points close to $m(-1)$ such that $u'(0; a_1, c_1)$ is close to -1 and $u'(0; a_2, c_2)$ close to 1, then this continuity property seems to imply that, for any fixed $d \in]-1, 1[$ there would exist (a, c) between (a_1, c_1) and (a_2, c_2) with $u'(0; a, c) = d$. In fact there is no contradiction: any small path joining (a_1, c_1) and (a_2, c_2) has to cross the “singular line” $\{(u_-(s), u'_-(s)) ; s < 0\}$ at some point (a_0, c_0) and the solution with this initial condition is no longer defined at 0. This could explain an error in [13] Lemma 2 p. 257, which asserts the continuity of \mathcal{L} .

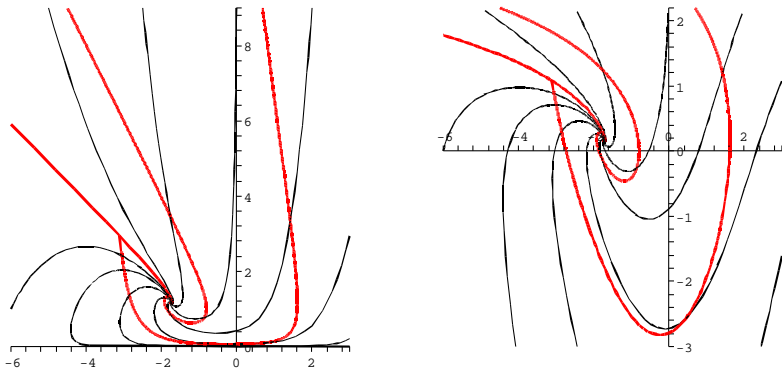


Figure 9: Numerical graphs of some orbits Γ_k and of the level set curves of the function \mathcal{L} . On the left nine curves Γ_k for various values of $k \in \mathbb{R} \cup \{\infty\}$ and $\mathcal{L}(a, c) = \lambda$ for $\lambda = 0, 1$ and 10. On the right the same curves in the plane $(a, \ln c)$, showing the details for small values of c . The flow of (12) transforms a level curve of $\mathcal{L}(a, c)$ into another level curve. Notice that the level set curve $\mathcal{L}(a, c) = 0$ is equal to the orbit Γ_∞ .

Proposition 6 shows that the discontinuity of \mathcal{L} at the point $m(-1)$ of Γ_∞ is equal to λ_+ , see [6] Theorem 2.5. The discontinuity of \mathcal{L} at any point $m(s)$ of Γ_∞ can be obtained using the similarity property (11). To see this, let $\Lambda(a, b, c)$ denote the limit, when $t \rightarrow \infty$, of the derivative $f'(t)$ of the

solution $f(t)$ of the BIVP

$$f''' + ff'' = 0, \quad f(0) = -a, \quad f'(0) = b, \quad f''(0) = c > 0.$$

This limit is finite and non negative ([6] Proposition 3.1). The function \mathcal{L} is simply given by

$$\mathcal{L}(a, c) = \Lambda(a, -1, c).$$

Then ([6] Proposition 2.1), $[-1, \Lambda(a, b, c)[$ is the maximal right interval of existence of the solution $u(s)$ of the CIVP

$$uu'' + s = 0, \quad u(b) = c > 0, \quad u'(b) = a.$$

The similarity property (11) implies

$$\forall \sigma > 0, \quad \Lambda(\sigma a, \sigma^2 b, \sigma^3 c) = \sigma^2 \Lambda(a, b, c). \quad (25)$$

This formula justifies, as said in the introduction, that the properties of Λ for $b < 0$ can be deduced from the case $b = -1$, i.e. from the properties of the function $\mathcal{L} : (a, c) \mapsto \Lambda(a, -1, c)$.

Notice that, for any positive solution u of the Crocco equation defined on some interval I , we have

$$\forall s \in I, \quad \mathcal{L}(u'(-1), u(-1)) = \Lambda(u'(-1), -1, u(-1)) = \Lambda(u'(s), s, u(s)).$$

As a consequence, (25) gives

$$\forall s < 0, \quad \mathcal{L}(u'(-1), u(-1)) = -s \mathcal{L}((-s)^{-1/2} u'(s), (-s)^{-3/2} u(s)).$$

In terms of the associated vector field, we deduce that for all (x, y) solution of (12)

$$\forall \tau \in \mathbb{R}, \quad \mathcal{L}(x(\tau), y(\tau)) = e^\tau \mathcal{L}(x(0), y(0)). \quad (26)$$

This formula shows how the τ -map flow of (12) transforms the level curve $\mathcal{L}(a, c) = \lambda$ into the level curve $\mathcal{L}(a, c) = e^\tau \lambda$, see Figure 9. Hence the similarity property (11) yields the discontinuity at any point of Γ_∞ .

Corollary 7 — The discontinuity of \mathcal{L} at a point $m(s)$ of Γ_∞ is as follows: on the convex side of Γ_∞ , \mathcal{L} tends to 0, whereas on the concave side, \mathcal{L} tends to $-\frac{\lambda_+}{s}$.

8 The number of solutions of the BBVP

To count the number of solutions of (5) we adopt the following strategy: for any values of $a \in \mathbb{R}$ and $\lambda \geq 0$, we count the number of values of c for which $\mathcal{L}(a, c) = \lambda$ where $\mathcal{L} : \mathbb{R} \times]0, +\infty[\rightarrow]0, +\infty[$ is the limit defined by (9). Let $A(\lambda)$ denote the abscissa of the point of Γ_∞ where \mathcal{L} takes the values 0 and

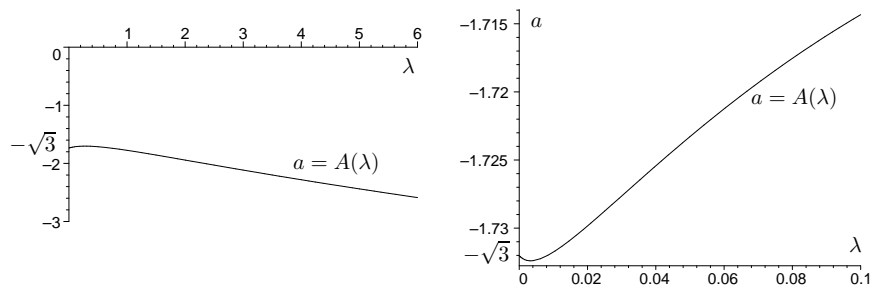


Figure 10: On the left: the graph of A . On the right: an enlargement near $(0, -\sqrt{3})$.

λ on each side of Γ_∞ respectively. Corollary 7 yields $-s = \frac{\lambda_\pm}{\lambda}$, from which we deduce that

$$A :]0, +\infty[\rightarrow]-\infty, 0[, \quad \lambda \mapsto \sqrt{\frac{\lambda}{\lambda_\pm}} u'_- \left(-\frac{\lambda_\pm}{\lambda} \right).$$

See Figure 10 for a numerical graph of A and Figure 12 for a sketch showing the oscillations near $\lambda = 0$. A careful study of the vector field shows that Γ_∞ has no inflexion point and S^* is a focus. Therefore for all $n \geq 1$, with the convention $a_0 = -\infty$, there exist functions

$$L_n : [a_{2n}, a_{2n-1}] \rightarrow \mathbb{R}, \quad R_n : [a_{2n-2}, a_{2n-1}] \rightarrow \mathbb{R},$$

L_n convex and R_n concave, such that Γ_∞ is the union of the graphs of the mappings $x \mapsto L_n(x)$ and $x \mapsto R_n(x)$; see Figure 3 right for the graphs of R_1 , R_2 and L_1 . As a consequence, the function A has the following properties.

Proposition 8 ([6] Proposition 1.1) — *The function A is C^∞ and has an infinite sequence of extremal points $(\lambda_n)_{n \geq 1}$ decreasing to 0: local minima at λ_{2n} and local maxima at λ_{2n+1} , and no other extremum. Let $A(\lambda_n) = a_n$ denote these extremal values. Sequences (a_{2n}) and (a_{2n+1}) are adjacent and*

$$\lim_{n \rightarrow +\infty} \frac{\lambda_{n+1}}{\lambda_n} = e^{-\pi\sqrt{2}}, \quad \lim_{n \rightarrow +\infty} \frac{a_{n+1} + \sqrt{3}}{a_n + \sqrt{3}} = -e^{-\pi\sqrt{2}}. \quad (27)$$

The map $\lambda \mapsto A(\lambda)$ is increasing on each interval $[\lambda_{2n}, \lambda_{2n-1}]$ and decreasing on each $[\lambda_{2n-1}, \lambda_{2n-2}]$.

Hence for all $n \geq 1$, with the convention $\lambda_0 = +\infty$, there exist one-to-one mappings

$$l_n : [a_{2n}, a_{2n-1}] \rightarrow [\lambda_{2n}, \lambda_{2n-1}], \quad r_n : [a_{2n-2}, a_{2n-1}] \rightarrow [\lambda_{2n-1}, \lambda_{2n-2}],$$

such that the graph of $\lambda \mapsto A(\lambda)$ is the union of the graphs of $a \mapsto l_n(a)$ and $a \mapsto r_n(a)$, see Figure 12 left for the graphs of r_1 , r_2 and l_1 .

Given $a \in \mathbb{R}$ and $\lambda \geq 0$, counting the number of solutions of the Blasius Problem (1-5) amounts to counting the number of times the function \mathcal{L} takes the value λ on a vertical ray

$$D_a := \{a\} \times]0, +\infty[. \quad (28)$$

For that purpose, we introduce the function

$$\mathcal{L}_a :]0, +\infty[\rightarrow]0, +\infty[, \quad c \mapsto \mathcal{L}(a, c).$$

The description below is succinct. We refer to [6] Section 2.4 for proofs, additional details and explanatory figures.

Let $n \geq 1$ be such that a is between a_{n-2} and a_n , possibly $a = a_n$ (with the convention $a_{-1} = +\infty$, $a_0 = -\infty$). Then the ray D_a crosses $n - 1$ times the spiral Γ_∞ (if $a = a_n$, there is an n -th point of contact but without crossing, hence without creating any discontinuity for \mathcal{L}_a). To fix ideas,

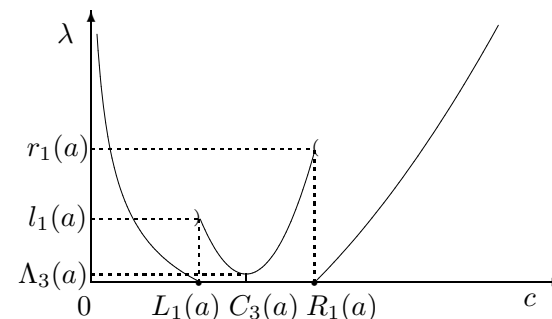


Figure 11: A sketch of graph of \mathcal{L}_a in the case $a_3 < a < a_1$, a close to a_3 .

assume that n is odd. A similar description can be done for n even. Then the graph of \mathcal{L}_a consists of n branches: $\frac{n-1}{2}$ on the left, one central and $\frac{n-1}{2}$ on the right. On the central part, by continuity, if a is close to a_n then \mathcal{L}_a has a minimum close to 0. Therefore we consider $d_n \in]a_n, a_{n-2}[$ as close to a_{n-2} as possible such that, for any $a \in [a_n, d_n[$, the central branch of \mathcal{L}_a attains its infimum, at some (possibly non unique) abscissa $c = C_n(a)$. We already know that $d_1 = +\infty$. For $n \geq 2$, let $\mu_n \in]\lambda_{n-1}, \lambda_{n-2}[$ be such that $d_n = A(\mu_n)$. For $a \in [a_n, d_n[$, we define $\Lambda_n(a)$ as the minimum of \mathcal{L}_a on its central branch. With the convention $\mu_1 = +\infty$, this yields a continuous map $\Lambda_n : [a_n, d_n[\rightarrow]0, \mu_n[$, satisfying $\Lambda_n(a_n) = 0$ and $\Lambda_n(a) \rightarrow \mu_n$ as $a \rightarrow d_n^-$. See Figure 11 for a sketch of graph of \mathcal{L}_a , Figure 13 for some graphs of \mathcal{L}_a when $a \approx a_1$ and Figure 14 for the graph of $\mathcal{L}_{-\sqrt{3}}$. We now present our main result.

Theorem 9 — The BBVP (5) has

- no solution if and only if $a > a_1$ and $0 \leq \lambda < \Lambda_1(a)$,
- at least n solutions (where $n > 0$) if (λ, a) belongs to one of the regions marked n in Figure 12, right, in other words, if:
 - either $a = A(\lambda)$ with $\mu_{n+1} \leq \lambda < \mu_n$,
 - or $\lambda = \Lambda_n(a)$ with $a \in [a_n, d_n[$ if n is odd, $a \in]d_n, a_n]$ if n is even, including the end-point $(0, a_n)$,
 - or (λ, a) is in the open region below the graphs of Λ_2 and A in the case $n = 1$, and in the open region between the graphs of $\Lambda_{n-1}, \Lambda_{n+1}$ and A in the case $n \geq 2$,
 - or $\lambda = 0$ and $a_{n-1} < a < a_{n+1}$ if n is odd, $a_{n+1} < a < a_{n-1}$ if n is even.
- infinitely many solutions if $\lambda = 0$ and $a = -\sqrt{3}$.

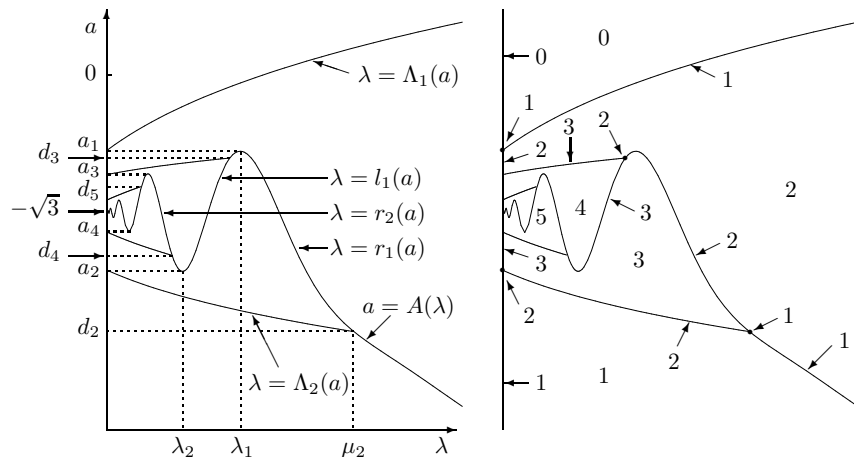


Figure 12: In the (λ, a) plane. On the left, a sketch of the graphs of the functions A and Λ_n ; on the right, a lower bound of the number of solutions of (5). We conjecture that this number is exact. We stress that the distances are not respected: due to (27) with $e^{\pi\sqrt{2}} \approx 85$, on the true graph of A no more than one extremal point is visible, see Figure 10.

Remark — We conjecture that each branch of \mathcal{L}_a is monotonous, except possibly the central one, which can be either monotonous or first decreasing then increasing, depending on the place of a with respect to the a_k and d_l . A consequence of this conjecture would be that this lower bound is tight.

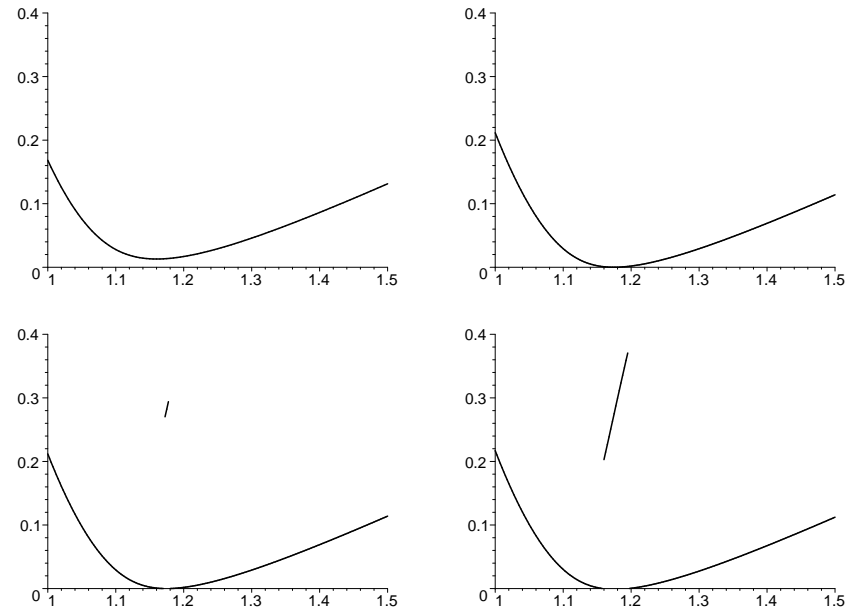


Figure 13: Scenario of bifurcation of the graphs of \mathcal{L}_a near $a_1 \approx -1.702704$. Top left: $a = -1.68$, top right: $a = -1.7027$, bottom left: $a = -1.7028$, bottom right: $a = -1.705$.

9 Numerical simulations

When (a, c) is close to Γ_∞ and on its concave side, $u(s; a, c)$ is exponentially small for the small negative value of s at which u reaches its minimum on $[-1, 0]$. This phenomenon can lead to bad numerical simulations. As we will see, the passage to the variables $s(v), w(v)$, corresponding to the variables $S(V), W(V)$ described in Section 5, is appropriate, not only for theoretical but also for numerical reasons. As an illustration, let us solve numerically, with the use of Maple, the CIVP (in the phase plane, i.e. with $v = u'$) with the initial conditions

$$\{(u(-1) = c_1 = 2.94, v(-1) = a = -3.12)\}$$

and

$$\{u(-1) = c_2 = 2.95, v(-1) = a\}.$$

The first initial condition lies on the concave side of Γ_∞ and the second one on its concave side. For the convenience of the reader we give hereafter the Maple instructions and the resulting output. Because the aim is to compute bounds of existence intervals of solutions, the output is an error message, with a numerical value of a possible singularity.

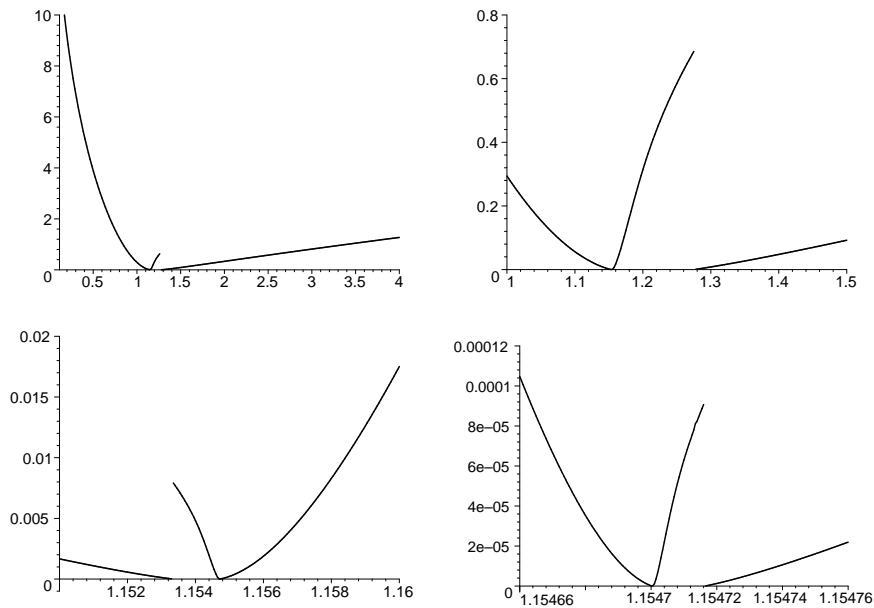


Figure 14: Numerical graph of \mathcal{L}_a for $a = -\sqrt{3}$, with successive enlargements.

```
> restart;
> a:=-3.12: c1:=2.94: c2:=2.95:
> EqCroccoUV:=diff(u(s),s)=v(s),diff(v(s),s)=-s/u(s):
```

$$\frac{du}{ds} = v, \quad \frac{dv}{ds} = -\frac{s}{u} \quad (29)$$

```
> SolCroccoUV:=proc(c)
>   Sol:=dsolve({EqCroccoUV,u(-1)=c,v(-1)=a},{u(s),v(s)},
>               numeric,output=listprocedure):
>   SolU:=eval(u(s),Sol):
>   SolU(50):
> end proc:
> SolCroccoUV(c1);
Error, (in SolU) cannot evaluate the solution further right of
-0.21850903e-2, probably a singularity
> SolCroccoUV(c2);
Error, (in SolU) cannot evaluate the solution further right of
0.99652635e-3, probably a singularity
```

The result for c_1 is not correct since the solution must be defined for all $s \leq 0$. The second result c_2 is correct and predicts that $\mathcal{L}(a, c_2) \approx 0.001$. It is a fact, not completely elucidated, that the use of the logarithmic change of variable $w = \ln u$ does not yield better numerical results: in the variables (w, v) the numerical solutions are still incorrect for c_1 (and correct for c_2).

```
> EqCroccoVW:=diff(w(s),s)=v(s)*exp(-w(s)),
>               diff(v(s),s)=-s*exp(-w(s));
```

$$\frac{dw}{ds} = ve^{-w}, \quad \frac{dv}{ds} = -se^{-w} \quad (30)$$

```
> SolCroccoVW:=proc(c)
>   Sol:=dsolve({EqCroccoVW,w(-1)=ln(c),v(-1)=a},{w(s),v(s)},
>               numeric,output=listprocedure):
>   SolW:=eval(w(s),Sol):
>   SolW(50):
> end proc:
> SolCroccoVW(c1);
Error, (in SolW) cannot evaluate the solution further right of
-0.21862961e-2, probably a singularity
> SolCroccoVW(c2);
Error, (in SolW) cannot evaluate the solution further right of
0.99531941e-3, probably a singularity
```

Following Section 5, we now consider the change of variable $w = \ln u$ and use the variable v as an independent variable. This gives correct numerical results.

```
> EqCroccoSW:=diff(s(v),v)=-exp(w(v))/s(v),diff(w(v),v)=-v/s(v);
```

$$\frac{ds}{dv} = -\frac{e^w}{s}, \quad \frac{dw}{dv} = -\frac{v}{s} \quad (31)$$

```
> SolCroccoSW:=proc(c)
>   Sol:=dsolve({EqCroccoSW,w(a)=ln(c),s(a)=-1},{w(v),s(v)},
>               numeric,output=listprocedure):
>   SolS:=eval(s(v),Sol):
>   SolS(10):
> end proc:
> SolCroccoSW(c1);
Error, (in SolS) cannot evaluate the solution further right of
2.7651840, probably a singularity
> SolCroccoSW(c2);
Error, (in SolS) cannot evaluate the solution further right of
-2.7726621, probably a singularity
```

We see that for c_1 , the solution $w(v)$ is computed until the value $v = 2.7651840$. Hence the numerical solution succeeded to pass exponentially close to the axis $u = 0$ and to reflect on this axis and get a positive derivative. The singularity encountered now at $v = 2.7651840$ is caused by the fact that system (31) is defined only in the half space $s < 0$. For $s \geq 0$ we must return to the original variables $u(s)$ and $v(s)$. Hence we use the following procedure to evaluate $\mathcal{L}(a, c)$.

```
> Lambda:= proc(a,c)
>   erreur:=0.0000000001:
>   fSW:=dsolve({EqCroccoSW,w(a)=ln(c),s(a)=-1},{s(v),w(v)},
>             numeric,stop_cond=[s(v)+erreur]):
>   fSW(10);
>   IC:=subs(%,[v,s(v),w(v)]):
>   v0:=IC[1]: s0:=IC[2]: w0:=IC[3]:
>   f:=dsolve({EqCroccoUV,u(s0)=exp(w0),v(s0)=v0},{u(s),v(s)},
>             numeric,stop_cond=[u(s)-erreur]):
>   f(50):
>   subs(% ,s):
> end proc:
```

This procedure is easy to understand. First system (31) is solved with initial conditions $w(a) = \ln(c)$, $s(a) = -1$ as far as $s \leq -\text{erreur}$. Next, one computes the values v_0 , $s_0 = s(v_0)$ and $w_0 = w(v_0)$ such that the stopping condition $s_0 = -\text{erreur}$ is reached. Then system (29) is solved with initial conditions $u(s_0) = e^{w_0}$, $v(s_0) = v_0$, as far as $u \geq \text{erreur}$. The procedure gives the value s_1 such that the stopping condition $u(s_1) = \text{erreur}$ is attained. This value is a very good approximation of $\mathcal{L}(a, c)$.

```
> Lambda(a,c1);
Warning, cannot evaluate the solution further right of
2.7651840, stop condition #1 violated
Warning, cannot evaluate the solution further right of
10.012058, stop condition #1 violated
10.0120586420604791
> Lambda(a,c2);
Warning, cannot evaluate the solution further right of
-2.7726621, stop condition #1 violated
Warning, cannot evaluate the solution further right of
.99606109e-3, stop condition #1 violated
0.000996061092810659674
```

Hence, $\mathcal{L}(a, c_1) \approx 10.012$ and $\mathcal{L}(a, c_2) \approx 0.001$. The following instructions which use the procedure `Lambda` produce the numerical graph of \mathcal{L}_a for $a = -\sqrt{3}$ and $1.15466 \leq c \leq 1.15476$, see Figure 14 bottom right.

```
> a:=-sqrt(3): c1:=1.15466: c2:=1.15476: N:=200;
> for n from 0 to N do LLambda[n]:=c1+n*(c2-c1)/N,
>             Lambda(a,c1+n*(c2-c1)/N) end do:
> L1:=[[LLambda[i]]$i=0..112]: L2:=[[LLambda[i]]$i=113..N]:
> plot([L1,L2],c1..c2,-.0000031..0.00012,thickness =4,
>       color=black);
```

References

- [1] Z. BELHACHMI, B. BRIGHI and K. TAOUS, On the concave solutions of the Blasius equation, *Acta Math. Univ. Comenianae* 69:2 (2000) 199-214.
- [2] E. BENOÎT Ed., *Dynamic Bifurcations*, Proceedings Luminy 1990, Lect. Notes Math. 1493 Springer-Verlag, 1991.
- [3] H. BLASIUS, Thesis, Göttingen (1907).
- [4] H. BLASIUS, Grenzsichten in Flüssigkeiten mit kleiner Reibung, *Zeitschr. Math. Phys.* 56 (1908) 1-37.
- [5] B. BRIGHI, Deux problèmes aux limites pour l'équation de Blasius, *Revue Math. Ens. Sup.* 8 (2001) 833-842.
- [6] B. BRIGHI, A. FRUCHARD and T. SARI, On the Blasius Problem, *Adv. Differential Equations* 13 (2008), no. 5-6, 509-600.
- [7] L. CROCCO, Sull strato limite laminare nei gas lungo una lamina plana, *Rend. Math. Appl. Ser. 5* 21 (1941) 138-152.
- [8] P. HARTMAN, *Ordinary Differential Equations*, Wiley, 1964.
- [9] M. Y. HUSSAINI and W. D. LAIKIN, Existence and non-uniqueness of similarity solutions of a boundary layer problem, *Quart. J. Mech. Appl. Math.* 39:1 (1986) 15-24.
- [10] M. Y. HUSSAINI, W. D. LAIKIN and A. NACHMAN, On similarity solutions of a boundary layer problem with an upstream moving wall, *SIAM J. Appl. Math.* 47:4 (1987) 699-709.
- [11] C. LOBRY, T. SARI and S. TOUHAMI, On Tykhonov's theorem for convergence of solutions of slow and fast systems, *Electron. J. Differential Equations* 19 (1998) 1-22.
- [12] O. A. OLEINIK, V. N. SAMOKHIN, *Mathematical Models in Boundary Layer Theory*, Applied Mathematics and Mathematical Computations 15, Chapman& Hall/CRC, Washington (1999)

- [13] E. SOEWONO, K. VAJRAVELU and R.N. MOHAPATRA, Existence and nonuniqueness of solutions of a singular non linear boundary layer problem, *J. Math. Anal. Appl.* 159 (1991) 251-270.
- [14] A. N. TIKHONOV, Systems of differential equations containing small parameters multiplying the derivatives, *Mat. Sb.* 31 (1952) 575-586.
- [15] W. WASOW, *Asymptotic Expansions for Ordinary Differential Equations*, Krieger, New York (1976).
- [16] H. WEYL, On the differential equations of the simplest boundary-layer problems, *Ann. Math.* 43 (1942) 381-407.

Address of the authors:

Laboratoire de Mathématiques, Informatique et Applications, EA3993
Faculté des Sciences et Techniques, Université de Haute Alsace
4, rue des Frères Lumière, F-68093 Mulhouse cedex, France

Current address for T. Sari:

EPI MERE INRIA/INRA, UMR MISTEA
SupAgro Bât 21, 2 Place Pierre Viala
F-34060 Montpellier cedex, France

E-addresses:

Bernard.Brighi@uha.fr, Augustin.Fruchard@uha.fr, Tewfik.Sari@uha.fr